

Soil degradation assessment across tropical grassland of Western Kenya

John N. Quinton^{1*}, Gabriel Yesuf², German Baldi³, Mengyi Gong⁴, Kelvin Kinuthia⁵, Ellen L. Fry⁶, Yuda Odongo⁷, Barthelemew Nyakundi⁷, Joseph Hitimana^{7†}, Patricia de Britto Costa⁶, Alice A. Onyango⁵, Sonja M. Leitner⁵, Richard D. Bardgett^{1,6}, Mariana C. Rufino^{8†}

¹Lancaster Environment Centre, Lancaster University, Lancaster, UK.

²Rural Payments Agency, Geospatial Services, Reading, UK

³Instituto de Matemática Aplicada San Luis –Universidad Nacional de San Luis & CONICET, San Luis, Argentina

⁴School of Mathematical Sciences, Lancaster University, Lancaster, UK

⁵Mazingira Centre for Environmental Research and Education, International Livestock Research Institute, Naivasha Rd, PO 30709, Nairobi, Kenya

⁶Department of Earth and Environmental Sciences, The University of Manchester, Oxford Road, Manchester, M13 9PT, UK.

⁷School of Agricultural Sciences and Natural Resources, University of Kabianga, P.O Box 2030 -20200. Kericho, Kenya

⁸Chair of Livestock Systems, TUM School of Life Sciences, Building 4308, Liesel-Beckmann Straße 4, Freising 85354, Germany

†deceased

*Correspondence to: John N. Quinton (J.Quinton@lancaster.ac.uk)

Abstract

Soils across sub-Saharan Africa are exposed to extensive degradation processes, which can reduce their ability to produce crops and support livestock. While there has been a significant research effort focussing on soil degradation in sub-Saharan croplands, less research effort had been directed towards grasslands. Here, we tested the effectiveness of remote sensing to classify the soil degradation status of smallholder grazing lands. Focussing on grasslands used by smallholders in the districts of Nyando and Kuresoi in Western Kenya, we first used remote sensing (RS) to classify grasslands as productive grazing lands, grazing lands that followed a variable trend in vegetation productivity (transition), and unstable and unproductive (degraded) grazing lands. We then tested how this classification related to measured soil parameters indicative of soil degradation. We then used this classification, which was based on a temporal analysis of Normalised Difference Vegetation Index (NDVI), Enhanced Vegetation Index (EVI) and Normalised Difference Water Index (NDWI) between 2013 and 2018, to identify 90 field sites across the two districts, which we then sampled and analysed for a range of physical, chemical and biological soil properties. Only soil microbial biomass carbon (C) showed consistent alignment with the RS classification, although there was some overlap with other soil parameters at one or other of the study areas. To group the sites using the soil variables, which we split by study area and into stable (those that are slow to change) and transient (those that change rapidly in response to a changing pedological environment), K-means clustering was undertaken. Two clusters were produced for each district. One of these clusters included sites with higher levels of C,

45 nitrogen (N), phosphorus (P) and pH, that aligned well with the RS classification at
Kuresoi, with seven out of ten productive sites being assigned to this cluster. The other
cluster included sites with high soil C and N, but low pH and relatively low soil bulk
density, and corresponded to 12 out of the 16 productive sites in Nyando. Overall, our
50 results suggest that while the use of RS methods for classifying degraded grasslands
and the soils supporting them does have significant advantages in terms of time and
costs over field survey, supplementing these methods with a limited set of soil
parameters related to nutrient cycling, such as microbial biomass C, soil P, percent C and
N, and soil pH, could enhance our ability to identify degraded soils and target
restoration efforts.

55 **Introduction**

Approximately 660 million hectares of sub-Saharan African (SSA) soils are estimated to
be degraded, which represents a significant portion of the global extent of degraded
soils (Gibbs and Salmon, 2015). Soil degradation reduces the functioning of soils and is a
60 result of multiple processes including soil erosion by wind, water and tillage,
salinisation, nutrient depletion, and compaction (Bridges and Oldeman, 1999) and may
be triggered by shifts in land use, management or climatic changes. Most attention has
been placed on the impacts of soil degradation on food security, and it has been cited as
the leading cause of stagnation in food production, creating uncertainties for income
and nutritional security for rural populations (Barbier and Hochard, 2016). Reduced
65 plant productivity associated with degraded soil also reduces the input of carbon (C) to
the soil leading to lower C stocks (Bai and Cotrufo, 2022) and less biomass to support
livestock. Further, when grazing lands are degraded, farmers are often forced to graze
their livestock in adjacent forests, which can negatively affect forest plant communities
(Mullah et al., 2023). Thus, restoring degraded soils has become a priority for securing
70 future food supply while simultaneously avoiding biodiversity and C losses. This has
resulted in several initiatives supporting landscape restoration in Africa, notably the
African forest restoration initiative (Messinger and Winterbottom, 2016), which
gathered commitments from African governments to restore 100 million hectares of
degraded land by 2030.

75 The East African highlands of Kenya are densely populated areas of high agro-ecological
potential. Farms here are small, typically smaller than 2 hectares (Lowder et al., 2016).
Production includes a mix of grains and vegetables for local consumption, some cash
crops, such as tea (*Camellia sinensis* (L.) O. Kuntze), and livestock keeping. Milk from
livestock is important to smallholder families as a valuable source of protein in a
80 protein-poor diet (Hulett et al., 2014). Grazing animals are also culturally significant,
reflecting the social standing of the owner and providing meat for celebrations and an
additional source of cash when sold (Moll, 2005). Smallholder systems in the highlands
of Kenya have a range of stocking rates, typically expressed in Tropical Livestock Units
(TLU) per hectare. Stocking rates in the Kenyan highlands are reported to be between 1
85 and 1.4 TLU ha⁻¹ depending on the nature of the system (Bebe et al 2003), whereas for
Murang'a County to the south east of our study area, they are 3-6 TLU ha⁻¹ (Ortiz-
Gonzalo et al, 2017) and for dairy cattle in Kiambu County to the west of our study area
an average of 2.1 TLU ha⁻¹ (Were et al 2025). Additionally, grazing takes place on farms
and on utility areas, which are controlled by local institutions; these often come under
90 higher greater pressure because multiple livestock owners have access to the land. In

response to these pressures, grassland soil degradation is widespread in Kenya (Nzau et al., 2018) although we know little about its extent and severity.

Given the importance of grazing land for sustaining rural livelihoods it is surprising that globally, and particularly in SSA, much less recent research attention has been placed on

95 understanding degradation of grazing lands (Bardgett et al., 2021). High grazing pressures can degrade soil fertility with associated declines in soil properties underpinning soil health (Pelster et al., 2017), for instance causing soil compaction and reducing soil infiltration rates (Owuor et al., 2018) and C inputs to soil due to the removal of plant material by livestock and reductions in root mass (Zhou et al., 2017).

100 Further, catchments with high livestock densities have larger nutrient and sediment loads in streams (Jacobs et al., 2017), have greater emissions of greenhouse gases (Arias-Navarro et al., 2017), and increase the risk of forest degradation (Brandt et al., 2018). Low soil nutrient availability and the deterioration in soil physical properties impairs plant growth and alters plant nutrient concentrations (Augustine et al., 2003), and reduces organic matter return to soil. With poorer vegetation cover and lower organic matter contents, soils become increasingly vulnerable to erosion, leading to lower soil depth and organic matter, which further reduces water and nutrient retention (Quinton and Fiener, 2024). This leads to a downward spiral of productivity loss and reduced capacity of systems to resist and recover from climate extremes (Van De Koppel et al., 1997; Quinton and Fiener, 2024).

110 The UN Decade (2021-30) on ecosystem restoration (Unep, 2019) has focused attention on understanding where and how severely soils are degraded and whether they can recover, which is clearly important for the design of restoration programmes. In grazed systems, soil degradation is often recognised by the presence of bare soil. However, using bare soil as an indicator can be problematic in systems where erratic rainfall patterns lead to seasonal and inter-annual fluctuations in vegetation growth coupled with reduced vegetation cover due to grazing (Ellis and Swift, 1988). In such environments, poor vegetation growth may or may not indicate degraded soils. However, utilising the response of vegetation to changed soil properties and water availability is an approach that has been used by several authors (e.g. Eckert et al., 2015; Zhou et al., 2017).

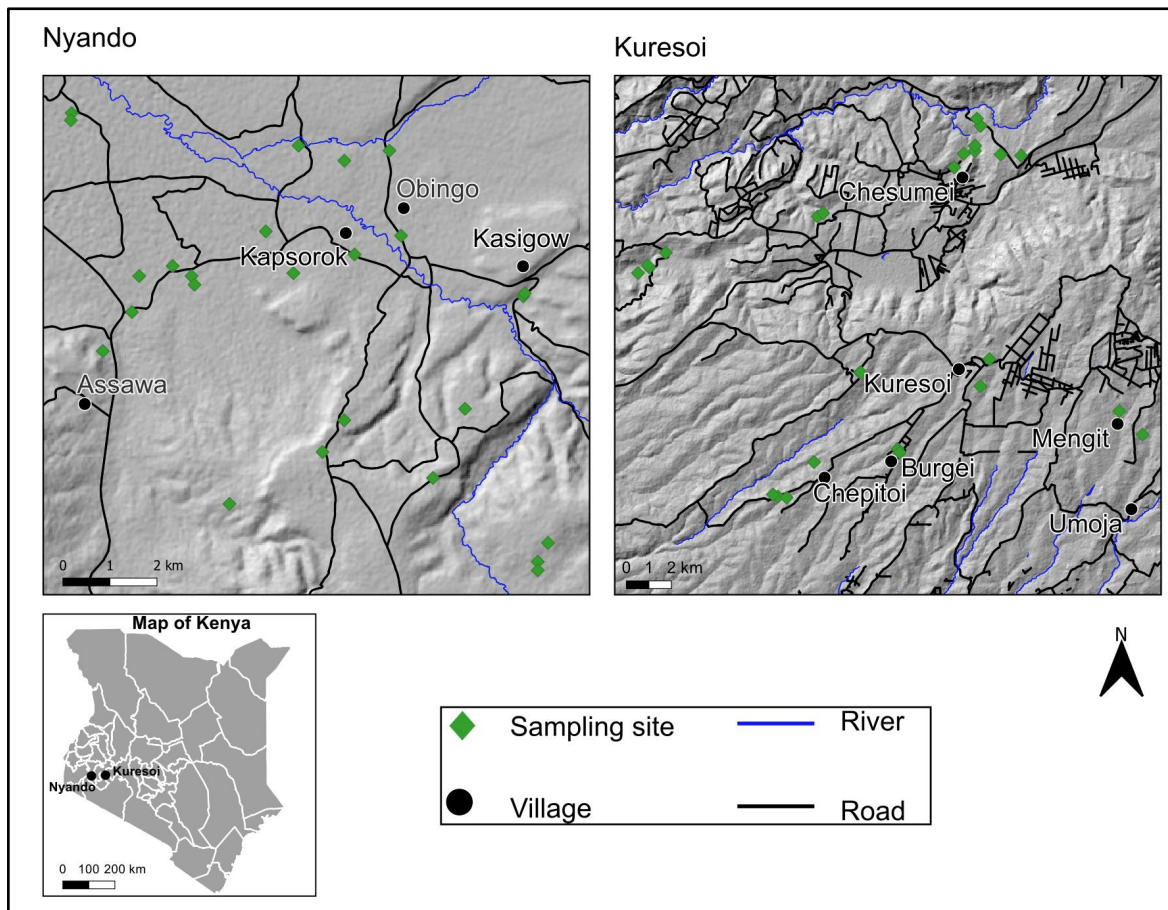
115 Here, we tested the reliability of remote sensing approaches for classifying degradation status of smallholder grazing land and compared it with an approach based on the sampling of soils and characterisation of soil properties related to soil structural stability and C, nitrogen (N) and phosphorus (P) cycling. Working in two areas representing smallholder grazing land of western Kenya (Nyando and Kuresoi), we assessed degradation using a dynamic multi-year approach to derive a range of metrics to quantify the magnitude, seasonality and interannual variability of the vegetation (Rufino et al., 2016), and then tested whether or not the classification was related to measured soil parameters. We then explored whether soil variables classified as either stable or transient could be used to classify soil degradation status in grasslands.

Methodology

Field areas

135 We used a comparative landscape-level analysis of two agro-ecosystems with different ecologies (Figure 1). The study areas are in western Kenya covering the neighbouring basins of the rivers Sondu-Miriu and Nyando spanning land use transitions from East African montane forests to grasslands and croplands. Study area 1 (Kuresoi) is in

140 Kericho county located in the Sondu river basin in the proximity of the Mau Forest, at an
 145 altitude ranging from 1,688 to 2947 masl, a mean slope of 7.6 degrees and a maximum
 150 of 29 degrees, with an average rainfall of 1,988±328 mm. The geology originates from
 the early Miocene, with phonolites dominating in the lower part of the catchment, and
 phonolitic nephelinites in the upper part. The topography is rolling with moderate
 slopes . A variety of Tertiary tuffs are found on the highest part of the Mau Escarpment
 (Jennings, 1971). Study area 2 is in Lower Nyando located in the Nyando river basin,
 with an average rainfall of 1,150 mm and spanning from the foot of a plateau at 1,781
 towards Lake Victoria at 1,170 masl, with a mean slope of 5.3 degrees and with a
 maximum slope of 21 degrees. Topography is gently sloping, towards ephemeral and
 permanent drainage. Soils are derived from Holocene alluvial deposits, and a variety of
 parent materials including phonolites and granitic gneisses (Iuss, 2015). The Lower
 Nyando study area covers an area which is approximately 160 km², whilst the Kuresoi
 study area covers an area that is approximately 1,300 km² next to the Mau Forest. More
 details on land use and vegetation are given below.



155 **Figure 1:** Location of study areas in Kenya (bottom left) and expanded views of Kuresoi
 (top right) and Lower Nyando (top left). Map produced using QGIS® software . Road
 network, river and settlement were reproduced using OpenStreetMap vector data.
 Accessed on 2019-06-09 and are licensed under the Open Database 1.0 License. Digital
 Elevation Model was produced using ASTER Global Digital Elevation Model (GDEM) 30-
 160 meter resolution as input and under license from NASA Earth Science Information
 Partners Data Preservation and Stewardship Committee. 2019. Earth Science Data. Ver.
 2.

Approach to degradation classification

165 Our approach to classifying grasslands focusses on the rate at which greening takes
place following a dry season (Yu et al., 2012) . We define productive grasslands are those
where biomass productivity is higher and returns rapidly following dry seasons. On the
other hand, degraded grasslands are those with lower peak biomass and which display
slow recovery following drought. Those grasslands that are intermediary, displaying
170 characteristics of both productive and degraded grasslands, are termed transition.
These states are defined using an analytical approach using remote sensing images of
both study areas which is set out in the following sections. This spatio-temporal analysis
covered a period of 5 years (2013 – 2018).

Remote sensing data selection

175 To analyse the structural characteristics of grasslands supporting smallholder
communities in Kuresoi and Lower Nyando, we implemented time-series seasonal
analysis that classified landscape-level stages of degradation. We used 35 satellite image
scenes from the archives of European Space Agency (ESA 2016) and United States
Geological Surveys (<https://earthexplorer.usgs.gov/>) (Table 1). The selection of different
sensors was necessary to: i) fill missing dates from the Sentinel collection which had the
180 higher spatial resolution, but shorter temporal resolution and ii) to maintain
consistency in annual seasonal sampling between 2013 and 2018. The final satellite
imagery was from Landsat-Thematic Mapper (TM) L2, Landsat Operational Land Imager
(OLI) L2 and Sentinel-2 sensors L2A. Level 2 images are Analysis Ready Data (ARD) and
atmospherically corrected surface reflectance and data and therefore free from the
185 effects of haze and water vapour. Landsat-TM and OLI imagery have a spatial resolution
of 30 m, while Sentinel-2 imagery has a spatial resolution of 10 m.

The decision to select and process high-resolution imagery is due to the focus on
smallholder dairy farms, which are associated with grazing lands that are often less than
190 1 ha and therefore easier to detect with higher resolution imagery. For LandSat-TM
scenes, we downloaded blue (band 1), red (band 3), near-infrared (band 4), and
shortwave infrared (band 6) spectral bands from USGS earth explorer repository. For
Landsat-OLI scenes, we downloaded blue (band 2), red (band 4), near-infrared (band 5)
and shortwave infrared (band 6). For the Sentinel-2 scenes, we downloaded blue (band
195 2), red (band 4), near infrared (band 8) and shortwave infrared (band 11). We loaded
the individual bands into RStudio using the raster package (R. All Landsat images were
resampled to 10 m using Sentinel-2 images as reference. This is because TIMESAT 3.3
(see description of use below), which is a program for analysing time-series of satellite
derived index data by extracting seasonal parameters (Eklundh and Jönsson, 2015) and
200 requires all input image scenes to have the same spatial resolution when creating raster
stacks and before model fitting. No further image enhancements were applied because
TIMESAT algorithm reduces negative biases arising from cloudiness by fitting the model
to the upper envelope of the vegetation/water index data (Eklundh and Jönsson, 2015).
Despite these corrections, TIMESAT is unable to reduce negatively biased residuals
205 related to surface anisotropy and sensor defects. However, we did not detect the effects
of sensor defects in this analysis. Afterwards, we calculated NDVI values in each pixel
by dividing the difference with the sum of near-infra red and red bands (Equation 1). To
derive EVI values in each pixel, we applied correction factors and divided the difference
between near-infrared and red bands with near-infrared band (Equation 2). We
210 calculated NDWI in each pixel by dividing the difference with the sum of near-infrared
and shortwave infrared (Equation 3).

Table 1: Summary of dates of acquisition of Landsat and Sentinel-2 imagery used for the determination of Normalized Difference Vegetation Index, Enhanced Vegetation Index and Normalized Difference Water Index.

215

	2013	2014	2015	2016	2017	2018
NA		2014/01/25 ¹	2015/01/12 ¹	2016/01/08 ²	2017/01/12 ²	2018/01/22 ²
	2013/04/28 ¹	2014/04/01 ¹	2015/04/02 ¹	2016/04/27 ²	2017/04/02 ²	2018/04/10 ¹
	2013/06/17 ¹	2014/06/18 ¹	2015/06/07 ¹	2016/06/06 ²	2017/06/11 ²	2018/06/11 ²
	2013/08/18 ¹	2014/08/21 ¹	2015/08/11 ²	2016/08/25 ²	2017/08/20 ²	2018/08/05 ²
	2013/10/05 ¹	2014/10/25 ¹	2015/10/25 ¹	2016/10/29 ¹	2017/10/29 ¹	2018/10/03 ¹
	2013/12/24 ¹	2014/12/11 ¹	2015/12/29 ²	2016/12/23 ²	2017/12/28 ²	2018/12/18 ²

¹ Landsat Thematic Mapper (TM) or Operational Land Imager (OLI) imagery

² Sentinel-2 imagery

Note: Landsat images were resampled to 10m resolution.

Temporal and seasonal analysis

220

Three vegetation indices, Normalised Difference Vegetation Index (NDVI), Enhanced Vegetation Index (EVI) and Normalised Difference Water Index (NDWI) were calculated using blue, red, near infra-red (NIR), and shortwave infra-red bands (Equations, 1, 2 and 3). These indices were selected because vegetation and water indices are effective to estimate changes in ecosystems (He et al., 2018) and grassland biomass (Todd et al., 1998), distinguish canopy density (Huete et al., 1997), and characterise drought (Rulinda et al., 2012).

225

$$NDVI = \frac{(NIR - Red)}{(NIR + Red)} \quad (1)$$

$$EVI = G * \left[\frac{(NIR - Red)}{(NIR + C1 * Red - C2 * Blue + L)} \right] \quad (2)$$

$$NDWI = \frac{(NIR - SWIR)}{(NIR + SWIR)} \quad (3)$$

230

where *NIR* is near-infra red; *G* represents a gain factor; *L* adjusts for canopy background; *C*₁ and *C*₂ are coefficients for atmospheric resistance (*G* = 2.5, *C*₁ = 6, and *C*₂ = 7.5). Applying these coefficients allows for index calculation as a ratio between Red and *NIR* values, while reducing the background noise, atmospheric noise, and data saturation. Index values were calculated on a scale of -1 to 1.

235

The seasonality of the vegetation was interpolated using TIMESAT v3.3 algorithm (Eklundh and Jönsson, 2015). An adaptive Savitzky-Golay smoothed function was fitted over the index time-series data of Lower Nyando to model bi-modal seasons and to determine the timings of the growing seasons. A double gaussian function was fitted over the index time-series data of Kuresoi to model seasonal peaks where the vegetation dynamics is less variable. The adaptive function of TIMESAT modelled abrupt changes in vegetation effectively, which was often the case in the Lower Nyando landscape consisting of an intricate mosaic of land covers. A double logistic function allowed to isolate noise (e.g. caused by clouds) in Kuresoi data. To capture seasonal peaks, the functions were fitted to the upper envelope of the time-series following Eklundh and Jönsson (2015).

240

245

Degradation units' classification

Five seasonal parameters were selected for the classification of degradation units: Start of Season (SoSv), Function value at End of Season (EoSv), Largest data, Maximum Value (MV), Greening rates (GR) and Browning rates (BR) because of the phenology characteristic of the ecosystems under study (Kong et al., 2022). For definitions of seasonal parameters and further explanations see (Eklundh and Jönsson, 2017). Productive vegetation state was expected to have higher values for SoSv, EoSv, MV and experience faster greening compared to vegetation of the units with transition and degraded states (Xiao et al., 2006; Yu et al., 2012). There are no predefined seasonal parameter values that define stages of grassland degradation in Western Kenya, as there are for other African grasslands (e.g. Tagesson et al. (2015) quantified maximum NDVI values between 0.59 and 0.82 for different grasslands in a semi-arid region of Senegal). The best performing two models from five tested, based on visually consistent classification and accurate spatial distribution of dominant land cover types (e.g., large forest patch). The thresholds used for selected seasonal parameters for each model are given in Table 2. Thresholding was implemented using written functions in R (R. Core Team, 2023) to partition parameter values into three groups corresponding to productive, transition, and degraded. All land cover types were retained during seasonal parameter estimation and classification to allow for accurate seasonal models of the study areas. Using the above approach and thresholds, productive vegetation was assigned to high MV (>0.8), high GR (>0.5), and low BR (<0.3). Vegetation at the degraded state had low MV (<0.5), low GR (≤ 0.8), and high BR (≥ 0.5) and transition grasslands were those falling between these values. Finally, the classification from each model was combined to determine areas of common agreement and produce maps identifying productive, transition, and degraded areas (Figure 2).

Table 2: Summary of models' description, seasonal parameters and threshold values used for degradation unit classification of Lower Nyando and Kuresoi.

275

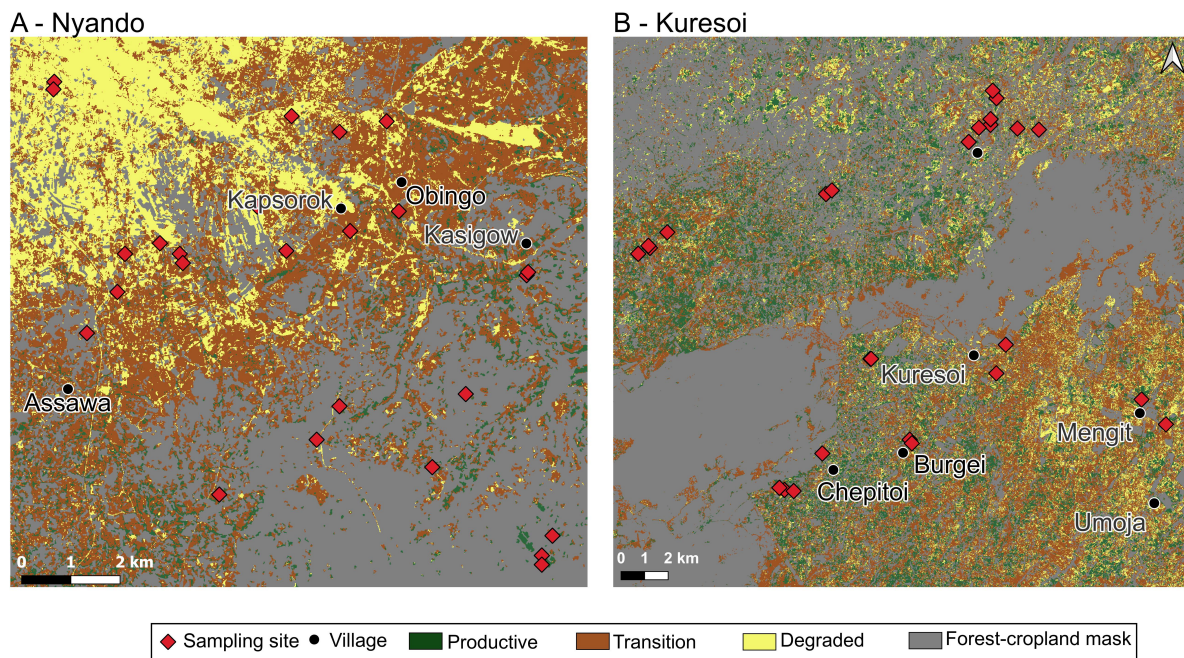
Description	Index	Threshold values (Nyando) [§]					Threshold values (Kuresoi) [§]				
		MV	SoSv	EoSv	GR	BR	MV	SoSv	EoSv	GR	BR
Model 1	EVI	0.49	0.50	0.49	0.54	0.54	0.75	0.76	0.76	0.79	0.74
	NDWI	0.81	0.79	0.79	0.77	0.81	0.83	0.82	0.82	0.79	0.80
Model 2	NDWI	0.81	0.79	0.79			0.83	0.82	0.82		

Selecting sampling locations

280

Land cover data from the European Space Agency Climate Change Initiative land cover vector layer (ESA 2016) was used to mask forests, urban and water bodies to detect grazing areas. Afterwards, locations were selected using the Fishnet tool of ArcGIS. Stratified random sampling was used to create sampling locations separated by a minimum distance of 1 km to select approximately 30 sampling locations for each degradation unit, resulting in 100 sampling locations including replacements. Locations land that coincided with recently cultivated areas (<10 years) and/or road tracks were removed following examination using Google Earth (2008 - 2018) . Locations that had signs of recent cultivation or tillage lines were excluded. In October-November 2019, the locations were visited to remove sample locations that were inaccessible or when landowners denied access. In total, 90 sites were selected for study (Figure 2).

285



290

Figure 2: Classification of Lower Nyando (A) and Kuresoi (B) study areas into three ERUs: productive, transition and regime-shift. Sampling sites are overlaid and show the distribution of field experiments and locations of soil and aboveground biomass samples. Map produced using QGIS® software . Settlement information were reproduced using OpenStreetMap vector data. Accessed on 2019-06-09 and are licensed under the Open Database 1.0 License. .

295 **Soil sampling and analyses**

Soils at each site were sampled to 10 cm depth and analysed for a range of physical, chemical and biological parameters (Table 3). For all analysis, unless stated, soils were air dried and ground to pass a 2 mm sieve prior to analysis.

300 Bulk density was calculated following sampling of intact soil with 45 mm diameter rings. Soil texture was determined by laser diffraction (Beckman-Coulter LSI3 320), after soil dispersion in sodium hexametaphosphate. Aggregate stability was determined using the fast-wetting method of aggregate stability (Le Bissonnais, 1996), which subjects the aggregates to rapid immersion in water for 10 min. After that, aggregate samples were sieved in ethanol before oven drying to determine final aggregate size
305 distribution, producing a mean weight diameter (MWD).

For each site sampled we measured total soil C, N, P, and selected microbial-mediated functions related to nutrient cycling. These were microbial biomass (C and N), nutrient availability (i.e. soluble inorganic and organic N and P pools, and dissolved organic C), rates of N mineralisation and nitrification. Briefly, percentage C and N in dry, ground soil
310 were measured using an elemental combustion analyser (Elementar Vario EL, Hanau, Germany). We measured dissolved total and organic C (DC and DOC respectively), plant available nitrate (NO_3^-) and total dissolved N (TDN) by weighing 5 g of fresh soil accurately and shaking in 35 ml Milli-Q water for 10 minutes at 150 rpm, before filtering through Whatman 42 filter paper. C in the filtrate was quantified using an Aurora
315 1030W TOC analyser (OI Analytical, UK), and N was quantified using an autoanalyser (AA3, Seal Analytical, Wrexham UK). Organic N was calculated by subtracting inorganic N values (nitrate and ammonium) from total N. pH of the filtrate was determined using a pH probe (Mettler Toledo FE20, Salford, UK). Values were adjusted for soil moisture.

320 Soil ammonium (NH_4^+) was measured by shaking 5 g of fresh soil in 25ml 1M KCl for 30 minutes, extracting through Whatman 1 filter paper and analysing on the autoanalyser as before. For potential mineralisation and nitrification, 5 g of each soil sample was incubated for 14 days at 25 °C before being extracted and analysed for NH_4^+ and NO_3^- using the KCl procedure. The values from the initial KCl extraction (summed NH_4^+ and NO_3^-) were subtracted from the day 14 extraction and divided by 14 to give a rate of
325 potential mineralisation per day. Nitrification was calculated by using the NO_3^- values only. Negative values imply denitrification, i.e. loss of N as N_2 gas. Microbial biomass C and N were determined using the chloroform-fumigation method (Vance 1987). We weighed 5 g of each sample twice. The first replicates were shaken in 25 ml 0.5M K_2SO_4 for 30 minutes, before passing through Whatman 42 filter paper. The second were
330 placed in a desiccator containing a beaker of chloroform under vacuum for 24 hours to lyse microbial cells, before being extracted as before. Total dissolved C and total extractable N were analysed using the Aurora and the autoanalyser respectively.

Microbial biomass C and N were calculated by subtracting the unfumigated values from the fumigated ones. Total soil P was measured using the Kjeldahl digestion method
335 (Kjeldahl, 1883). We mixed 420 ml concentrated sulfuric acid with 12 g lithium sulphate. We added 0.5 ml of this mixture to 50 mg of dry ground soil per sample in glass digestion tubes. We then added 0.5 ml 30% hydrogen peroxide. Samples were heated at 200°C, then we added a 50°C heat increase every 30 minutes until it reached 360°C. Samples were heated at 360°C for two hours before cooling. When cool, 0.5ml of
340 hydrogen peroxide was added and samples were digested at 360°C for a further two hours. Samples were diluted to 50 ml using Milli-Q water. They were analysed using the ascorbic acid microplate method after (Kuo, 1996), where samples were measured colourimetrically at 880 nm. For inorganic P, we placed 2g of dry soil into a falcon tube

345 with 50ml of 0.5M sulfuric acid. This was shaken at 150rpm for 16 hours. The samples were centrifuged at 1500 rpm for 10 minutes, and the supernatant was analysed using the ascorbic acid method (Olsen and Sommers, 1982).

350 In addition, a suite of extracellular enzyme activities involved in the degradation of cellulose, chitin, lignin and proteins (i.e. β -glucosidase (GLC), cellobiohydrolase (CBH), β -xylosidase (XYL), N-acetylglucosaminidase (NAG), phosphatase (PHO), phenol oxidase (POX), peroxidase (PER), and urease (URE)), were determined which added artificial p-nitrophenyl (pNP) linked substrates to induce a colour reaction through p-nitrophenyl production following Fry et al. (2018) and De Vries and Bardgett and as described in Broadbent et al. (2022).

Description of the data set

355 For testing and clustering analysis, we focused on a total of 28 soil variables measured from the soil samples collected from the 0-0.1m depth in Kuresoi and Nyando. These variables were grouped in relation their rate of change in response to degradation as either stable (changes over multi-year time periods) or transient (changes over seasonal time periods) soil variables

360 Bulk density and soil hydraulic properties change over multi-annual, timescales (Berisso et al., 2012), as can contents of C (Tully et al., 2015), N (Sun and Chen, 2025) and P along with pH (Tully et al., 2015), and thus were considered stable. Other soil physical variables (percentage sand, silt, and clay, and aggregate stability) were also considered stable. We reason that that as aggregate stability is strongly related to soil texture and
365 organic matter (Kemper and Koch, 1966) both variables that change slowly, that aggregate stability will also change slowly, although there is little literature evidence to support this. In contrast, soil biological parameters, including enzyme activities, microbial biomass, and rates of nutrient mineralisation, respond rapidly to change in response to seasonal changes environmental conditions (Cordero et al., 2023) and therefore soil enzymes (PHO, GLC, NAG, XYL, CBH, PER, POX, URE), water extractable
370 NO_3 , and KCl-extracted NH_4 , microbial C, microbial N, total dissolved C, organic dissolved C, mineralisation and nitrification were considered transient.

The statistical analysis for investigating the difference between degradation classes were carried out on the 28 variables across all 45 sites in Kuresoi and Nyando
375 respectively. For the clustering analysis, the sites with incomplete data (i.e., with missing observation in any of the variables in the stable or transient variable sets) were removed, resulting in 31 sites in Nyando, 41 sites in Kuresoi for the stable variables, and 42 sites in Nyando, 38 sites in Kuresoi for the transient variables. The number of sites in each degradation class is given in Table 3.

380 Statistical analysis of field data

Statistical analyses were carried out to investigate differences in field sampling data between sites with different degradation labels allocated from remote sensing (Table 2). The analyses were applied to the data from Kuresoi and Nyando respectively. First,
385 analysis of variance (ANOVA), with the soil variables being the response and the degradation class labels being the explanatory variable, was applied to soil variables which follow approximately a normal distribution, according to Shapiro-Wilks test. This is to identify any mean differences between the degradation classes. For variables that failed the normality test (i.e., having more than one degradation classes that are not normally distributed), the non-parametric Kruskal-Wallis test was used. For soil
390 variables with a significant mean difference, further pairwise comparison tests were

applied to each pair of degradation classes (i.e., productive vs. degraded, productive vs transition, transition vs. degraded). Tukey's honest significant difference (HSD) test was used for parametric testing and Wilcoxon rank test was used for non-parametric testing.

Description of the clustering methods

395 Considering the features of our data sets, i.e., relatively large number of variables (12
and 16 for stable and transient variables respectively) as compared to the number of
sites (between 31 to 42) in each area, relatively high variability in some variables, and
initial experiments with different clustering methods, we chose to use k-means
clustering for our main analysis. In particular, the k-means clustering was applied to the
400 principal components extracted from the data. Below we briefly introduce the
clustering method and provide some details on the approach we took.
K-means clustering is a popular method for grouping a population of n subjects (n being
the number of sites in this case), each of p -dimensional (p being the number of
covariates), into a number of k clusters, using algorithms developed by e.g. Lloyd
405 (1957); Macqueen (1967); Hartigan and Wong (1979). Fraley and Raftery (2002) Few
assumptions are required for applying the k-means algorithm, although it has been
acknowledged that the method works better with clusters that are of similar shapes or
sizes (Steinley, 2006). The result can be sensitive to outliers (Johnson and Wichern,
2007). To determine the number of clusters for k-means clustering, methods such as
410 elbow plot of the total sum of squared distance between points and cluster centres and
gap statistics (Tibshirani et al., 2001) can be used. (Scrucca et al., 2023), To begin with,
principal component analysis (PCA) was applied to reduce the dimension of the data.
The number of principal components (PCs) was selected to account for at least 80% of
the variation in the data. This resulted in six PCs each for the clustering of stable and
415 transient variables from Kuresoi and Nyando respectively, which helped to improve the
stability of the clustering algorithms. Due to the relatively small population size in this
analysis, only cluster numbers from two to five were investigated. Based on the model
selection criteria, after taking the robustness of the clustering results into account and
discounting the cluster numbers that resulted in singletons (i.e., one site as a group of its
420 own), the cluster number was settled to be two for both stable and transient soil
variable sets in Kuresoi and Nyando.

The k-means clustering analysis was implemented in R (R. Core Team, 2023) using the
"mclust" package (Scrucca et al., 2023). Investigation of the clustering results was
425 carried out in R using the "fossil" package (Vavrek, 2011).

Results

Relation of remote sensing classification to measured soil parameters

Table 3 reports the mean and standard deviation for the soil variables measured in the
two study areas and identifies those variables that showed significant differences
430 between degradation states, which are then plotted in Figure 3. Microbial biomass C
and soil bulk density were the only two variables that showed significant differences
($p < 0.1$) between degradation classes at both areas. There was a significant increase
($p < 0.05$) of 74% in mean microbial biomass C from degraded sites to productive sites at
Kuresoi, and a significant increase ($p < 0.05$) of 70% at Nyando. Although the differences
435 between the transition and degraded/productive sites were not significant, the rankings
of the class means were consistent (degraded < transition < productive) for both areas.

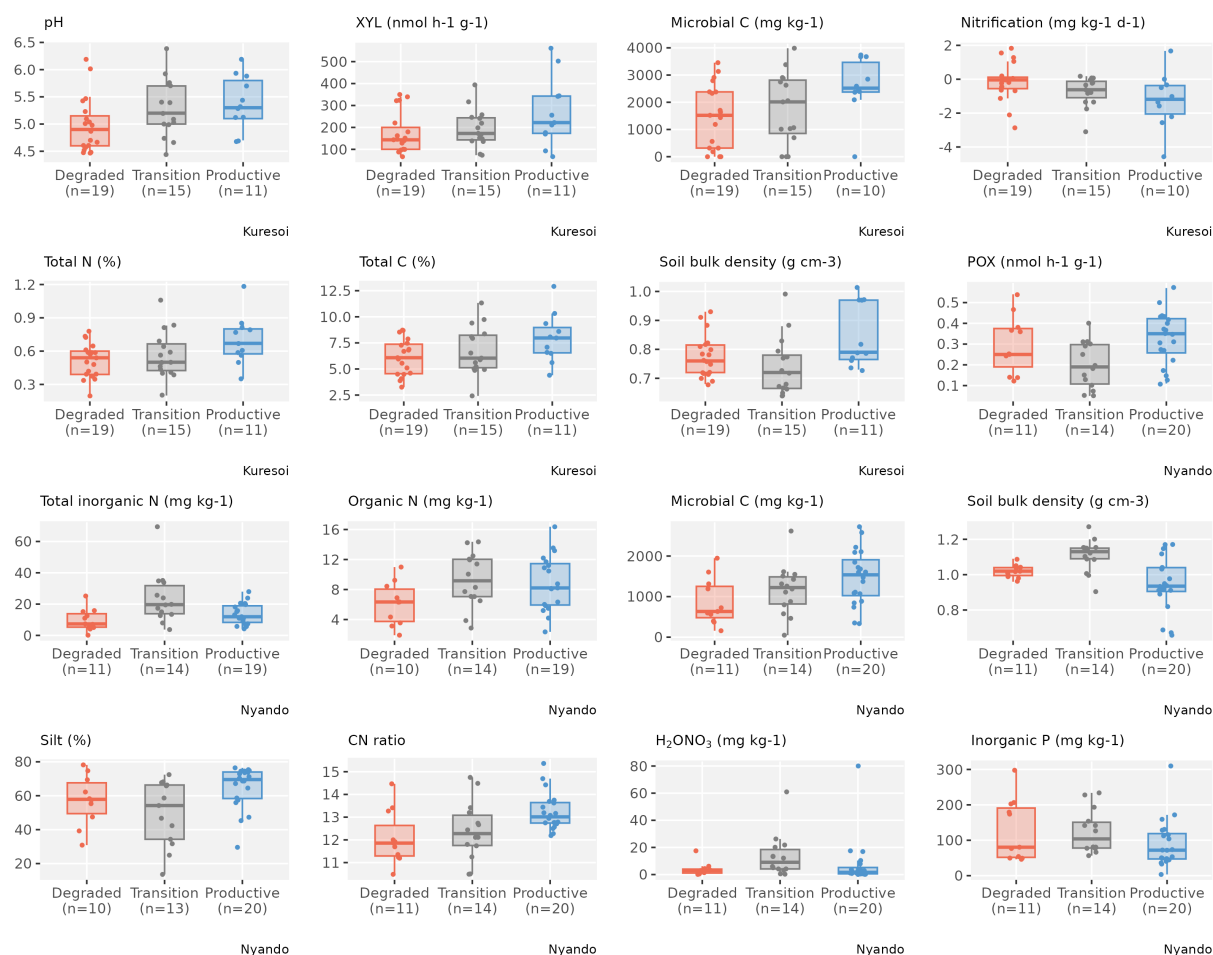
The largest difference in soil bulk density was seen between the transition class and the productive class for both Kuresoi ($p < 0.05$) and Nyando ($p < 0.05$). In this case, the rankings are inconsistent, with productive > degraded > transition at Kuresoi and transition > degraded > productive at Nyando, although the absolute differences between the classes were small (c.f. 0.1 g cm^3). Of the other soil variables that showed significant differences between degradation classes within each area: pH, total N and C and XYL at Kuresoi and C:N ratio at Nyando ranked the classes in the order degraded < transition < productive; inorganic P ranked the classes in the order of degraded > transition > productive, but the difference between degraded and transition is insignificant. Specifically, at Kuresoi, mean pH increased by 0.4 from the degraded to productive class, mean total C increased from 6.1% to 7.9%, mean total N from 0.5% to 0.7%, and mean XYL increased by 54%, from 172.9 to 267.6 $\text{nmol h}^{-1} \text{g}^{-1}$ dry soil. At Nyando, soil C:N ratio increased from 12.1 in the degraded class to 13.2 in the productive class.

Table 3. Mean and standard deviation (in brackets) of 28 soil variables (top 0-10 cm) by degradation labels measured at field sites in the two study areas, Kuresoi and Nyando, along with the significance level of the between label differences from ANOVA (where * represents $p < 0.1$, and ** represents $p < 0.05$). Variables that show a significant difference between degradation classes at the $p < 0.1$ level as determined by a pairwise t-test are designated by a different letter in parenthesis.

Variable	Kuresoi				Nyando			
	Degraded	Transitio	Productiv	ANOVA	Degrade	Transitio	Producti	ANOVA
	n	n	e		d	n	ve	
<i>Stable variables</i>								
pH	5.0 ±0.5 (a) (n=19)	5.3±0.5 (b) (n=15)	5.4±0.5 (b) (n=11)	*	5.8±0.9 (n=10)	5.4±0.6 (n=14)	5.6±0.8 (n=20)	
Total inorganic N (mg kg ⁻¹)	21.7±14.8 (n=19)	21.0±13.4 (n=15)	31.7±18.9 (n=11)		9.9±7.0 (a) (n=11)	23.7±16.3 (b) (n=14)	13.6±6.7 (a) (n=19)	* *
Organic N (mg kg ⁻¹)	7.2±4.1 (n=19)	8.0±3.3 (n=15)	8.1±3.3 (n=11)		6.1±2.9 (a) (n=10)	9.3±3.6 (b) (n=14)	8.9±3.7 (b) (n=19)	*
Inorganic P (mg kg ⁻¹)	131.4±147.5 (n=19)	82.7±67.7 (n=15)	70.9±82.5 (n=11)		128.8±86.4 (ab) (n=11)	124.1±60.2 (a) (n=14)	90.4±68.7 (b) (n=20)	*
Total P (mg kg ⁻¹)	1093.4±568.3 (n=19)	1176.1±631.2 (n=15)	1328.2±729.3 (n=11)		660.2±421.5 (n=10)	457.0±188.0 (n=13)	523.3±367.9 (n=19)	
Total N (%)	0.5±0.1 (a) (n=19)	0.6±0.2 (ab) (n=15)	0.7±0.2 (b) (n=11)	*	0.2±0.1 (n=11)	0.3±0.1 (n=14)	0.3±0.1 (n=20)	
Total C (%)	6.1±1.7 (a) (n=19)	6.8±2.3 (ab) (n=15)	7.9±2.3 (b) (n=11)	*	2.8±1.3 (n=11)	4.1±1.4 (n=14)	3.8±1.9 (n=20)	
Soil bulk density (g cm ⁻³)	0.8±0.1 (ab) (n=19)	0.7±0.1 (a) (n=15)	0.8±0.1 (b) (n=11)	* *	1.0±0.0 (a) (n=11)	1.1±0.1 (b) (n=14)	0.9±0.1 (c) (n=20)	* *
Aggregate stability Mean weight diameter (µm)	314.1±54.3 (n=18)	321.3±62.6 (n=15)	312.0±40.9 (n=10)		279.2±56.7 (n=5)	234.2±111.9 (n=11)	245.5±119.5 (n=17)	
Sand (%)	7.8±9.6 (n=18)	9.3±11.0 (n=15)	11.7±8.6 (n=10)		18.6±18.5 (n=10)	22.7±20.7 (n=13)	15.4±15.4 (n=20)	
Silt (%)	60.7±12.4 (n=18)	63.1±9.9 (n=15)	63.0±7.0 (n=10)		57.3±15.0 (ab) (n=10)	49.8±19.0 (a) (n=13)	65.0±12.5 (b) (n=20)	* *

Clay (%)	31.4±14.5 (n=18)	27.6±11.1 (n=15)	25.3±8.8 (n=10)	24.1±13.8 (n=10)	27.5±20.8 (n=13)	19.5±8.1 (n=20)	
CN ratio	12.0 ± 1.1 (n=19)	12.1 ± 0.8 (n=15)	11.5 ± 0.7 (n=11)	12.1 ± 1.2 (a) (n=11)	12.4 ± 1.3 (a) (n=14)	13.2 ± 0.8 (b) (n=20)	* *
CP ratio	76.8 ± 56.3 (n=19)	74.6 ± 45.3 (n=15)	120.1 ± 166.4 (n=11)	83.9 ± 105.2 (n=10)	125.6 ± 109.7 (n=13)	98.5 ± 62.1 (n=19)	
NP ratio	6.5 ± 5.0 (n=19)	6.1 ± 3.7 (n=15)	10.4 ± 14.3 (n=11)	7.3 ± 9.8 (n=10)	10.5 ± 9.8 (n=13)	7.6 ± 4.9 (n=19)	
<i>Transient variables</i>							
N NAG (nmol h ⁻¹ g ⁻¹ dry soil)	82.2±41.0 (n=19)	99.3±56.5 (n=15)	83.4±44.4 (n=11)	78.4±45.5 (n=11)	97.7±40.3 (n=14)	72.5±30.2 (n=20)	
XYL (nmol h ⁻¹ g ⁻¹ dry soil)	172.9±92.6 (a) (n=19)	196.0±86.2 (ab) (n=15)	267.6±157.1 (b) (n=11)	197.8±86.9 (n=11)	259.2±166.5 (n=14)	175.2±148.9 (n=20)	* *
CBH (nmol h ⁻¹ g ⁻¹ dry soil)	34.3±11.0 (n=18)	42.7±14.6 (n=15)	41.9±23.6 (n=11)	33.5±27.2 (n=11)	36.4±26.0 (n=14)	44.4±47.2 (n=20)	
PER (nmol h ⁻¹ g ⁻¹ dry soil)	11.1±14.4 (n=19)	8.9±8.5 (n=15)	6.9±7.4 (n=11)	4.1±3.0 (n=11)	3.2±1.9 (n=14)	4.8±2.6 (n=20)	
POX (nmol h ⁻¹ g ⁻¹ dry soil)	0.3±0.2 (n=19)	0.3±0.3 (n=15)	0.2±0.2 (n=11)	0.3±0.1 (a) (n=11)	0.2±0.1 (b) (n=14)	0.3±0.1 (a) (n=20)	* *
URE (nmol h ⁻¹ g ⁻¹ dry soil)	8.7±5.7 (n=19)	6.9±6.1 (n=15)	10.5±6.8 (n=11)	8.0±7.5 (n=11)	12.3±8.9 (n=14)	7.3±5.8 (n=20)	
KClNH ₄ (mg kg ⁻¹)	9.5±17.5 (n=19)	8.1±7.4 (n=15)	9.3±13.7 (n=11)	7.0±4.6 (n=11)	9.4±9.3 (n=14)	8.5±7.0 (n=20)	
H ₂ ONO ₃ (mg kg ⁻¹)	13.3±14.4 (n=19)	12.3±11.5 (n=15)	22.4±18.8 (n=11)	3.9±4.9 (n=11)	13.6±15.9 (b) (n=14)	7.8±17.8 (a) (n=20)	* *
Microbial C (mg kg ⁻¹)	1486.7±171.9 (a) (n=19)	1760.0±310.0 (ab) (n=15)	2583.0±095.6 (b) (n=10)	863.6±568.0 (a) (n=11)	1167.7±618.6 (ab) (n=14)	1471.4±676.2 (b) (n=20)	* *
Microbial N	109.9±53.7 (n=19)	126.8±92.5 (n=15)	171.2±107.1 (n=11)	67.1±40.2 (n=11)	95.3±56.9 (n=14)	84.0±50.0 (n=20)	

(mg kg ⁻¹)	(n=15)	(n=15)	(n=9)	(n=11)	(n=14)	(n=18)
Dissolved Total C	267.7±73. 2	296.3±85. 7	288.1±96. 5	293.3±9 5.9	319.3±8 2.4	338.8±1 52.2
(mg kg ⁻¹)	(n=19)	(n=15)	(n=11)	(n=10)	(n=14)	(n=20)
Dissolved Organic C	263.7±73. 3	293.3±86. 8	283.4±93. 5	269.0±8 3.3	301.5±7 1.7	322.6±1 45.1
(mg kg ⁻¹)	(n=19)	(n=15)	(n=11)	(n=10)	(n=14)	(n=20)
Mineralis ation	0.2±1.1 (n=19)	-0.0±0.8 (n=15)	-0.5±1.6 (n=10)	-0.2±1.0 (n=11)	-0.2±3.3 (n=14)	0.6±0.6 (n=20)
(mg kg ⁻¹ d ⁻¹)						
Nitrificat ion	-0.1±1.1 (n=19)	-0.7±0.9 (n=15)	-1.2±1.7 (n=10)	-0.2±1.1 (n=11)	-0.1±2.7 (n=14)	-0.1±0.7 (n=20)
(mg kg ⁻¹ d ⁻¹)						



460

Figure 3: Box and whisker plots of the soil variables with significant difference between degradation classes based on ANOVA or Kruskal-Wallis test from Kuresoi and Nyando respectively. The coloured dots are observations overlaid on top of the box plots.

465

Which stable and transient soil variables explain the clustering of soils in the two study areas?

Table 4 summarises the number of sites in Kuresoi and Nyando that have been grouped into two clusters by the k-means algorithm for stable and transient variables. Note that the total number of sites used in the clustering analysis for each area is different.

470

Table 4: Number of degraded, transition and productive sites allotted to two clusters at Kuresoi and Nyando using K-means clustering for stable and transient variables.

	Kuresoi		Nyando	
	Cluster 1	Cluster 2	Cluster 1	Cluster 2
<i>Stable variables</i>				
Degraded	8	9	2	3
Transition	8	7	4	6
Productive	2	7	4	12
Total	18	23	10	21
<i>Transient variables</i>				
Degraded	4	10	2	8
Transition	6	9	8	6
Productive	6	3	5	13
Total	16	22	15	27

475

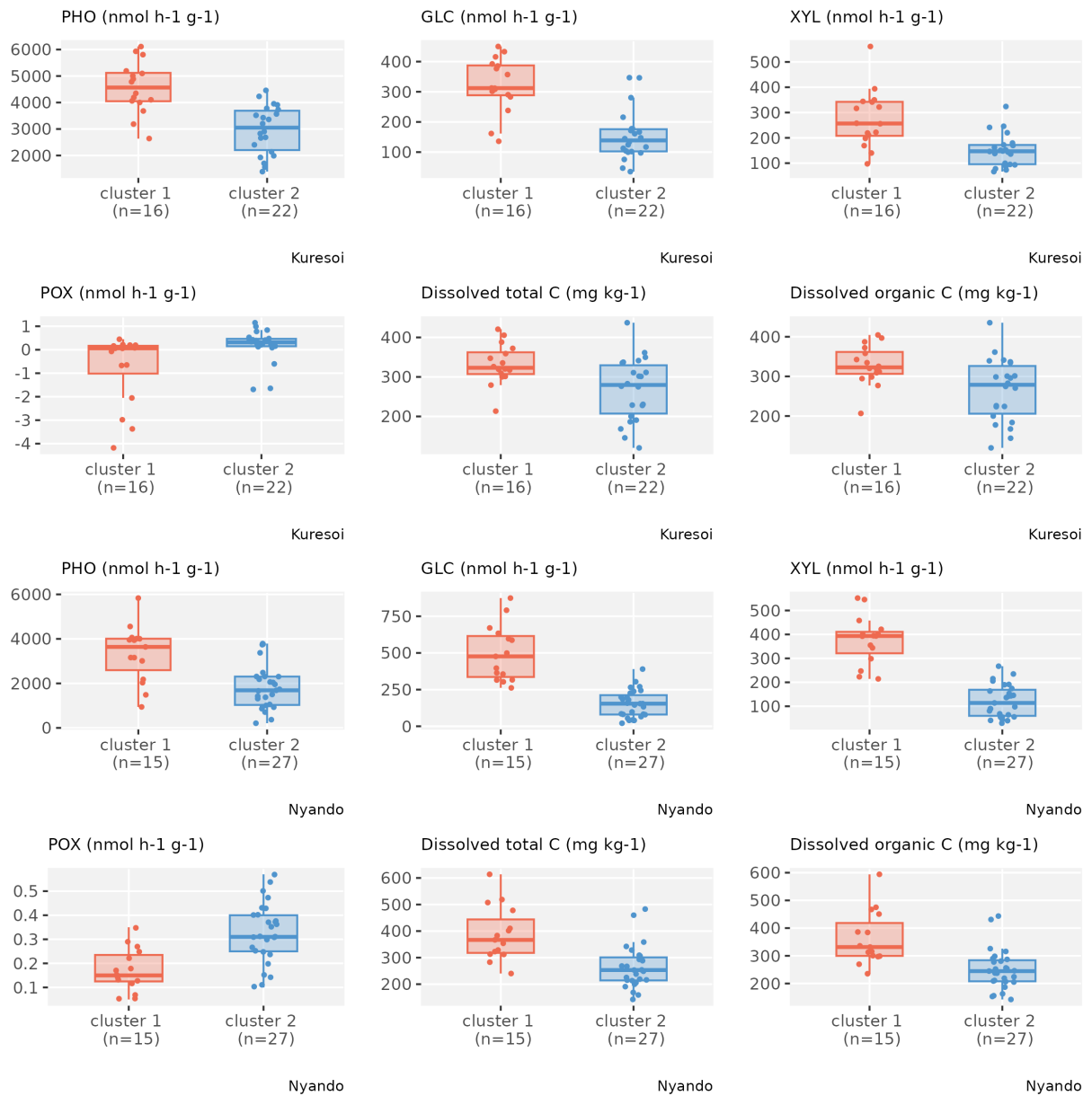
For the stable variables, in Kuresoi, sites in cluster 2 had significantly higher values of total N, total inorganic N, organic N, total P, total C and pH (significant at 0.05 level under two-sample t-tests). There was a significant difference in silt and clay contents of the two clusters. From Table 4, we see that 7 out of 9 Kuresoi productive sites, from the remote sensing classification, were assigned to cluster 2, but the numbers of transitional and degraded sites were distributed evenly between two clusters. Similarly, in Nyando, one cluster (cluster 2) had higher levels of total P, total N and total C, but lower pH and relatively low soil bulk density (all significant at $p < 0.05$ level). There was a significant difference in sand, silt and clay percentages. In total, 12 out of 16 productive sites in Nyando were assigned to this cluster. The transitional and degraded sites appeared to be equally likely in two clusters. For the transient variables, in Kuresoi, sites in one cluster (cluster 1) tended to have higher PHO, GLC, XYL, CBH, but lower POX. It also had higher microbial N, nitrate (extracted in $H_2O NO_3$), microbial C, total dissolved C. In Nyando, one cluster (cluster 1) consisted of sites with higher PHO, GLC, XYL, NAG, total dissolved C, but lower PER and POX. The cluster labels did not match the degradation labels in both cases. This is not surprising as the transient variables are highly variable and can change substantially in a short period of time. Box plots showing how the two clusters differed in selected stable (Figure 4) and transient (Figure 5) variables are given for Kuresoi and Nyando. All variables shown in the figures have significant mean difference at $p < 0.05$ level under a two-sample t-test.

480

485

490

495



500

Figure 4: Box and whisker plots of selected stable variables that show a significant mean difference ($p < 0.05$) between two clusters in both Kuresoi and Nyando, with observations (coloured dots) overlaid on top.

505



510 Figure 5: Box and whisker plots of selected transient variables that show a significant mean difference ($p < 0.05$) between two clusters in both Kuresoi and Nyando, with observations (grey dots) overlaid on top.

515 To further investigate the features of the clusters, we evaluated the inter-quantile range (IQR) between the 0.15 and 0.85 quantiles of the samples from sites allocated to each cluster, representing the spread of about 70% of the samples. For stable variables in Kuresoi, the IQRs of the samples from sites allocated to cluster 1 are 401 to 1091 (mg kg^{-1}) for total P, 0.35% to 0.50% for total N, and 3.98% and 5.76% for total C. Whereas the IQRs of the sites allocated to cluster 2 are 893 to 2024 (mg kg^{-1}) for total P, 0.56% to 0.82% for total N, and 6.55% and 9.64% for total C. In Nyando, the sites allocated to cluster 1 have IQRs of 181 to 503 (mg kg^{-1}) for total P, 0.11% to 0.21% for total N and 1.58% to 2.92% for total C. The sites allocated to cluster 2 have IQRs of 307 to 1226 (mg kg^{-1}) for total P, 0.23% to 0.49% for total N and 3.38% to 6.38% for total C. Overall, the clustering analysis grouped the sites with higher or lower total N and total C relatively

520

525 well, with the IQRs show clear difference between two clusters. However, there are some overlaps between the IQRs of total P from two clusters for both Kuresoi and Nyando. For the transient variables, we see mostly overlapping IQRs between clusters, with the exception of GLC in Kuresoi, and GLC, XYL in Nyando.

Discussion

530 The ability of remote sensing to classify degradation status over large areas (e.g. Cordell et al., 2017; Manić et al., 2022; Wang et al., 2024), at relatively low cost and utilising data that can be rapidly updated as new images become available, is an attractive proposition, since it provides land managers, policy makers and scientists with a mechanism for targeting interventions. Combined remote sensing and measurement of
535 soil properties has been used to map soils in Africa with some success (Vågen et al., 2016). Nevertheless, there have been relatively few attempts to compare remotely sensed classification against soil data collected from soil sampling programmes. Our work demonstrates that, while it is relatively straightforward to generate classifications using derived parameters, such as NDVI, NDWI and EVI, that reflect vegetation
540 dynamics, the resulting classification only reflected changes in a few in-situ soil parameters related to soil degradation.

Across the two studied districts (i.e., Nyando and Kuresoi) we detected consistent alignment between remote sensing classification of degradation and microbial biomass C, a key soil biological parameter related to nutrient and C cycling processes in soil
545 (Tate, 2017) that is tightly linked to plant diversity and productivity (Chen et al., 2019) and is known to respond quickly (c.100 days) to inputs of fresh organic matter to soil, including plant litter and animal wastes (Dai et al., 2021b). Therefore, it is likely that we are seeing the soil response to the amount of litter, root exudates, and dung from grazing animals, that is returned to the soil, all of which are functions of above-ground biomass reflected in the dynamics of NDVI. Apart from microbial biomass C, only bulk density showed differences related to degradation in both study areas, although the rankings were inconsistent and inter-site differences small. There was little consistent agreement between the remotely sensed classification with other field-based soil variables (Table 2). Some variables considered good proxy indicators for soil health and
555 which correlate with other important soil functions (Lal, 2016), such as C and N concentrations, C:N ratio and pH, were statistically significant for one site, but not the other.

We see two problems with the use of RS classification of soil degradation in the western Kenyan environment. First is the difficulty associated with unravelling the effect of
560 rainfall variability and soil degradation as observed remotely (Wessels et al., 2007), whereby it may be difficult to distinguish the role of drought and degradation. These difficulties are compounded in the context of smallholder farming due to grazing occurring on small parcels of land where plant biomass is variable and depends not only on soil and rainfall, but upon frequency and intensity of grazing. Thus, in these
565 situations, counter-intuitive results are possible. For example, following a drought it is likely that grazing takes place on the most resilient and rapidly recovering areas (the productive and transitional sites in this study) rather than those that are slow to revegetate (the degraded sites), potentially resulting in misclassification of productive conditions as degraded. Second, as the RS was used to plan the soil survey, it meant that
570 the RS images did not coincide with the survey dates. However, given that we used RS

data to consider seasonal shifts in vegetation indices over six years (Table 1), we do not think that an additional year of data would have changed our findings.

The clustering had some overlap with the productive sites in both areas and therefore provides an indication of a reduced number of soil properties that could be used to guide targeting efforts for restoration. The cluster analysis revealed some consistent patterns within the soil data and some agreement between the clustering and the classification derived from remote sensing with seven out of nine and 12 out of 16 productive sites attributed to the same cluster at Kuresoi and Nyando, respectively. These higher nutrient status clusters were characterised by higher soil N, P and C contents in both study areas, suggesting that these clusters are more fertile. This was supported by the separation between the inter-quantile ranges for total N and total P in both study areas. pH was also an important variable in the two clusters in both study areas, but with lower pHs featuring in the Nyando study area and higher pHs at Kuresoi. This reflects the different soils present in the two areas: soils at Nyando are prone to salinisation and tend to have a higher overall pH compared to the more acidic soils at Kuresoi, so it appears that what we are seeing in the 'productive' clusters is the inclusion of more favourable, slightly acid pHs in both study areas. Of the transient variables, the enzymes PHO, GLC and XYL featured in the higher nutrient status clusters in both study areas. Both GLC and XYL are key for breaking down cellulose and releasing energy for the soil microbial community, while PHO plays an important role in releasing P from organic matter for plant uptake (Jackson et al., 2013).

Our data, although extensive in terms of soil chemical and biological parameters, only considered one soil physical variable, aggregate stability, and thus provides limited insights into the physical condition of the soils. It is possible that the inclusion of infiltration rates and water holding capacity into our measurements may have produced a better relationship between RS and soil properties related to degradation. Work in China demonstrated a reduction in water holding capacity with increasing levels of degradation classified using grassland species composition (Yi et al., 2012), and hydraulic conductivity was shown to decline with degradation, defined by vegetation parameters (Zeng et al., 2013). However, more recent studies, using shrub coverage as the basis for degradation classification, report less clear relationships between soil water parameters and degradation (Dai et al., 2021a).

Conclusion

Remote sensing was able to map grassland degradation over large areas of western Kenya and offers the potential for cost-effective and dynamic monitoring. However, when the RS classification was compared to measured soil variables, apart from microbial C, soil C and N in one or other of the study areas, agreement was generally poor. This is probably due to the highly heterogeneous smallholder grazing lands in Nyando and Kuresoi. Here, vegetation cover and greenness is affected by variations in livestock grazing pressure as well as soil degradation status, resulting in only limited agreement with measured soil values.

The statistical clustering produced two clusters in each of the areas based on stable and transient or dynamic soil properties. The clusters for each of the study areas largely reflected differences in nutrient status and biogeochemical cycling, with one cluster at each area having higher soil N, P, and C contents and greater activities of selected extracellular enzymes (i.e., PHO, GLC and XYL); seven out of nine and 12 out of 16 productive sites attributed to this cluster at Kuresoi and Nyando, respectively. In addition, separation between the inter-quantile ranges between the clusters in both

620 study areas was found for total soil N and C. Thus, when assessing soil degradation in
grazed smallholder farming settings we propose sampling a small additional set of soil
variables that pertain to biogeochemical cycling (soil microbial C, total C and total N) to
provide confidence for identifying degraded soils and helping to target restoration
efforts.

Author contributions

625 JQ and MR led the writing of the paper, MR led the study and secured the funding for the
work, along with RDB, JH and JQ. All authors contributed to the manuscript. In addition,
GY and GB carried out the remote sensing analysis and contributed to the data analysis,
MG carried out data analysis, KK, EF, YO, BN PDB, AO collected field data.

Acknowledgements

630 We acknowledge funding from the UK Biotechnology and the Biological Sciences
Research Council (UKRI-BBSRC), through the Global Challenges Research Fund (GCRF)
under Agri-systems research to enhance rural livelihoods in developing countries [grant
number BB/S014934/1]. SML and KK acknowledge the CGIAR trust fund for funding
received through the Science Programmes Climate Action, Multifunctional Landscapes,
635 and Sustainable Farming.

Data and code availability

The code for the remote sensing analysis is available at
<https://github.com/GabYESUF/ReDEAL.git>

Dedication

640 We dedicate this paper to Mariana Rufino and Joseph Hitimana, committed scientists
and educators and critical to the success of this work who sadly both died before this
paper could be published.

References

- 645 Arias-Navarro, C., Díaz-Pinés, E., Zuazo, P., Rufino, M. C., Verchot, L. V., and
Butterbach-Bahl, K.: Quantifying the contribution of land use to N₂O, NO and CO₂
fluxes in a montane forest ecosystem of Kenya, *Biogeochemistry*, 134, 95-114, 2017.
Augustine, D. J., McNaughton, S. J., and Frank, D. A.: Feedbacks between soil
nutrients and large herbivores in a managed savanna ecosystem, *Ecological*
650 *Applications*, 13, 1325-1337, 2003.
Bai, Y. and Cotrufo, M. F.: Grassland soil carbon sequestration: Current
understanding, challenges, and solutions, *Science*, 377, 603-608, 2022.
Barbier, E. B. and Hochard, J. P.: Does land degradation increase poverty in
developing countries?, *PloS one*, 11, e0152973, 2016.
655 Bardgett, R. D., Bullock, J. M., Lavorel, S., Manning, P., Schaffner, U., Ostle, N.,
Chomel, M., Durigan, G., L Fry, E., and Johnson, D.: Combatting global grassland
degradation, *Nature Reviews Earth & Environment*, 2, 720-735, 2021.
Berisso, F. E., Schjønning, P., Keller, T., Lamandé, M., Etana, A., de Jonge, L. W.,
Iversen, B. V., Arvidsson, J., and Forkman, J.: Persistent effects of subsoil
660 compaction on pore size distribution and gas transport in a loamy soil, *Soil and*
Tillage Research, 122, 42-51, <https://doi.org/10.1016/j.still.2012.02.005>, 2012.
Brandt, M., Wigneron, J.-P., Chave, J., Tagesson, T., Penuelas, J., Ciais, P.,
Rasmussen, K., Tian, F., Mbow, C., and Al-Yaari, A.: Satellite passive microwaves

665 reveal recent climate-induced carbon losses in African drylands, *Nature ecology & evolution*, 2, 827-835, 2018.

Bridges, E. and Oldeman, L.: Global assessment of human-induced soil degradation, *Arid soil research and rehabilitation*, 13, 319-325, 1999.

Broadbent, A. A., Bahn, M., Pritchard, W. J., Newbold, L. K., Goodall, T., Guinta, A., Snell, H. S., Cordero, I., Michas, A., and Grant, H. K.: Shrub expansion modulates
670 belowground impacts of changing snow conditions in alpine grasslands, *Ecology Letters*, 25, 52-64, 2022.

Chen, C., Chen, H. Y. H., Chen, X., and Huang, Z.: Meta-analysis shows positive effects of plant diversity on microbial biomass and respiration, *Nature Communications*, 10, 1332, 10.1038/s41467-019-09258-y, 2019.

675 Cordell, S., Questad, E. J., Asner, G. P., Kinney, K. M., Thaxton, J. M., Uowolo, A., Brooks, S., and Chynoweth, M. W.: Remote sensing for restoration planning: how the big picture can inform stakeholders, *Restoration Ecology*, 25, S147-S154, <https://doi.org/10.1111/rec.12448>, 2017.

Cordero, I., Leizeaga, A., Hicks, L. C., Rousk, J., and Bardgett, R. D.: High intensity perturbations induce an abrupt shift in soil microbial state, *The ISME Journal*, 17, 2190-2199, 10.1038/s41396-023-01512-y, 2023.

Dai, L., Guo, X., Ke, X., Du, Y., Zhang, F., and Cao, G.: The variation in soil water retention of alpine shrub meadow under different degrees of degradation on
685 northeastern Qinghai-Tibetan plateau, *Plant and Soil*, 458, 231-244, 10.1007/s11104-020-04522-3, 2021a.

Dai, W., Peng, B., Liu, J., Wang, C., Wang, X., Jiang, P., and Bai, E.: Four years of litter input manipulation changes soil microbial characteristics in a temperate mixed forest, *Biogeochemistry*, 154, 371-383, 10.1007/s10533-021-00792-w, 2021b.

690 Eckert, S., Hüsler, F., Liniger, H., and Hodel, E.: Trend analysis of MODIS NDVI time series for detecting land degradation and regeneration in Mongolia, *Journal of Arid Environments*, 113, 16-28, 2015.

Eklundh, L. and Jönsson, P.: TIMESAT: A software package for time-series processing and assessment of vegetation dynamics, in: *Remote Sensing Time Series*, Springer, 141-158, 2015.

695 Eklundh, L. and Jönsson, P.: TIMESAT 3.3 software manual, Lund and Malmö University, Lund, Sweden, 2017.

Ellis, J. E. and Swift, D. M.: Stability of African Pastoral Ecosystems: Alternate Paradigms and Implications for Development, *J. Range Manage.*, 41, 450-459, 10.2307/3899515, 1988.

700 Fraley, C. and Raftery, A. E.: Model-Based Clustering, Discriminant Analysis, and Density Estimation, *Journal of the American Statistical Association*, 97, 611-631, 2002.

Gibbs, H. K. and Salmon, J. M.: Mapping the world's degraded lands, *Applied Geography*, 57, 12-21, <http://dx.doi.org/10.1016/j.apgeog.2014.11.024>, 2015.

705 Hartigan, J. A. and Wong, M. A.: Algorithm AS 136: A K-Means Clustering Algorithm, *Journal of the Royal Statistical Society. Series C (Applied Statistics)*, 28, 100-108, 1979.

He, M., Kimball, S. J., Maneta, P. M., Maxwell, D. B., Moreno, A., Beguería, S., and Wu, X.: Regional Crop Gross Primary Productivity and Yield Estimation Using Fused
710 Landsat-MODIS Data, *Remote Sensing*, 10, 2018.

Huete, A. R., HuiQing, L., and Leeuwen, W. J. D. v.: The use of vegetation indices in forested regions: issues of linearity and saturation, *IGARSS'97. 1997 IEEE*

- International Geoscience and Remote Sensing Symposium Proceedings. Remote Sensing - A Scientific Vision for Sustainable Development, 1966-1968,
- 715 Hulett, J. L., Weiss, R. E., Bwibo, N. O., Galal, O. M., Drorbaugh, N., and Neumann, C. G.: Animal source foods have a positive impact on the primary school test scores of Kenyan schoolchildren in a cluster-randomised, controlled feeding intervention trial, *The British Journal of Nutrition*, 111, 875–886, 2014.
- IUSS: World reference base for soil resources 2014. Update 2015. International soil classification system for naming soils and creating legends for soil maps. World Soil Resources Reports No. 106, FAO, Rome 2015.
- 720 Jackson, C. R., Tyler, H. L., and Millar, J. J.: Determination of Microbial Extracellular Enzyme Activity in Waters, Soils, and Sediments using High Throughput Microplate Assays, *Journal of Visualized Experiments : JoVE*, 80, 10.3791/50399, 2013.
- 725 Jacobs, S. R., Breuer, L., Butterbach-Bahl, K., Pelster, D. E., and Rufino, M. C.: Land use affects total dissolved nitrogen and nitrate concentrations in tropical montane streams in Kenya, *Science of The Total Environment*, 603-604, 519-532, <https://doi.org/10.1016/j.scitotenv.2017.06.100>, 2017.
- Jennings, D. J.: *Geology of the Molo area* (No. 86). 1971.
- 730 Johnson, R. A. and Wichern, D. W.: *Applied Multivariate Statistical Analysis*, Pearson Prentice Hall, U.S. 2007.
- Kemper, W. D. and Koch, E. J.: Aggregate stability of soils from Western United States and Canada: Measurement procedure, correlations with soil constituents, 1355, *Agricultural Research Service, US Department of Agriculture* 1966.
- 735 Kjeldahl, J.: Neue Methode zur Bestimmung des Stickstoffs in organischen Körpern, *Zeitschrift für analytische Chemie*, 22, 366-382, 10.1007/BF01338151, 1883.
- Kong, D., McVicar, T. R., Xiao, M., Zhang, Y., Peña-Arancibia, J. L., Filippa, G., Xie, Y., and Gu, X.: phenofit: An R package for extracting vegetation phenology from time series remote sensing, *Methods in Ecology and Evolution*, 13, 1508-1527, 2022.
- 740 Kuo, S.: Phosphorus: Ascorbic acid method, in: *Methods of Soil Analysis, Part 3. Chemical Methods*, SSSA Book Series, SSSA, ASA, Madison, USA, 909, 1996.
- Lal, R.: Soil health and carbon management, *Food and Energy Security*, 5, 212-222, <https://doi.org/10.1002/fes3.96>, 2016.
- 745 Le Bissonnais, Y.: Aggregate stability and assessment of soil crustability and erodibility .1. Theory and methodology, *European Journal Of Soil Science*, 47, 425-437, 1996.
- Lloyd, S. P.: *Least squares quantization in PCM*, Bell Lab, 1957.
- Lowder, S. K., Scoet, J., and Raney, T.: The number, size, and distribution of farms, smallholder farms, and family farms worldwide, *World development*, 87, 16-29, 2016.
- 750 MacQueen, J.: Some methods for classification and analysis of multivariate observations, *Proceedings of the Fifth Berkeley Symposium on Mathematical Statistics and Probability*,
- Manić, M., Đorđević, M., Đokić, M., Dragović, R., Kićović, D., Đorđević, D., Jović, M., Smičiklas, I., and Dragović, S.: Remote Sensing and Nuclear Techniques for Soil
- 755 Erosion Research in Forest Areas: Case Study of the Crveni Potok Catchment, *Frontiers in Environmental Science*, Volume 10 - 2022, 10.3389/fenvs.2022.897248, 2022.
- Messinger, J. and Winterbottom, B.: African forest landscape restoration initiative (AFR100): restoring 100 million hectares of degraded and deforested land in Africa, 2016.
- 760 Moll, H. A. J.: Costs and benefits of livestock systems and the role of market and nonmarket relationships, *Agricultural Economics*, 32, 181–193, 2005.

Mullah, J. A., Ngonga, B. O., and Bii, W.: The impact of livestock grazing on forest structure, ground flora and regeneration of disturbed areas in Mau Forest, Kenya Forestry Research Institute Nairobi, Kenya 2023.

765 Nzau, M., Mwangi, S. W., and Kinyenze, J. M.: Degradation of Grassland Ecosystems, Climate Change and Impacts on Pastoral Communities in Kenya, African Multidisciplinary Journal of Research, 3, 2018.

Olsen, S. R. and Sommers, L. E.: Phosphorus, in: Methods of Soil Analysis, 403-430, <https://doi.org/10.2134/agronmonogr9.2.2ed.c24>, 1982.

770 Owuor, S. O., Butterbach-Bahl, K., Guzha, A., Jacobs, S., Merbold, L., Rufino, M. C., Pelster, D. E., Díaz-Pinés, E., and Breuer, L.: Conversion of natural forest results in a significant degradation of soil hydraulic properties in the highlands of Kenya, Soil and tillage Research, 176, 36-44, 2018.

775 Pelster, D., Rufino, M., Rosenstock, T., Mango, J., Saiz, G., Diaz-Pines, E., Baldi, G., and Butterbach-Bahl, K.: Smallholder farms in eastern African tropical highlands have low soil greenhouse gas fluxes, Biogeosciences, 14, 187-202, 2017.

Quinton, J. N. and Fiener, P.: Soil erosion on arable land: An unresolved global environmental threat, Progress in Physical Geography: Earth and Environment, 48, 136-161, 2024.

780 R. Core Team: R: A Language and Environment for Statistical Computing, 2023.

Rufino, M. C., Atzberger, C., Baldi, G., Butterbach-Bahl, K., Rosenstock, T. S., and Stern, D.: Targeting landscapes to identify mitigation options in smallholder agriculture, Methods for Measuring Greenhouse Gas Balances and Evaluating Mitigation Options in Smallholder Agriculture, 15-36, 2016.

785 Rulinda, C. M., Dilo, A., Bijker, W., and Stein, A.: Characterising and quantifying vegetative drought in East Africa using fuzzy modelling and NDVI data, Journal of Arid Environments, 78, 169-178, 2012.

Scrucca, L., Fraley, C., Murphy, T. B., and Raftery, A. E.: Model-Based Clustering, Classification, and Density Estimation Using mclust in R, Chapman and Hall/CRC, 10.1201/9781003277965, 2023.

790 Steinley, D.: K-means clustering: A half-century synthesis, British Journal of Mathematical and Statistical Psychology, 59, 1-34, 10.1348/000711005X48266, 2006.

795 Sun, S. and Chen, S. S.: Extensive Decline of Soil Nitrogen and Its Drivers in the Lake Victoria Basin of Tropical Africa (1996–2015), Land Degradation & Development, 36, 5911-5926, <https://doi.org/10.1002/ldr.70045>, 2025.

Tagesson, T., Fensholt, R., Guiro, I., Rasmussen, M. O., Huber, S., Mbow, C., Garcia, M., Horion, S., Sandholt, I., Holm-Rasmussen, B., Götsche, F. M., Ridler, M. E., Olén, N., Lundegard Olsen, J., Ehammer, A., Madsen, M., Olesen, F. S., and Ardö, J.: Ecosystem properties of semiarid savanna grassland in West Africa and its relationship with environmental variability, Global Change Biology, 21, 250-264, 2015.

800 Tate, K. R.: Microbial Biomass: A Paradigm Shift in Terrestrial Biogeochemistry, WORLD SCIENTIFIC (EUROPE), 348 pp., doi:10.1142/q0038, 2017.

Tibshirani, R., Walther, G., and Hastie, T.: Estimating the Number of Clusters in a Data Set Via the Gap Statistic, Journal of the Royal Statistical Society Series B: Statistical Methodology, 63, 411-423, 10.1111/1467-9868.00293, 2001.

810 Todd, S. W., Hoffer, R. M., and Milchunas, D. G.: Biomass estimation on grazed and ungrazed rangelands using spectral indices, International Journal of Remote Sensing, 19, 427-438, 1998.

- Tully, K., Sullivan, C., Weil, R., and Sanchez, P.: The State of Soil Degradation in Sub-Saharan Africa: Baselines, Trajectories, and Solutions, *Sustainability*, 7, 6523-6552, 2015.
- 815 United Nations decade on ecosystem restoration 2021-2030:
<https://www.decadeonrestoration.org/>, last access: 23/4/2025.
- Vågen, T.-G., Winowiecki, L. A., Tondoh, J. E., Desta, L. T., and Gumbricht, T.: Mapping of soil properties and land degradation risk in Africa using MODIS reflectance, *Geoderma*, 263, 216-225,
820 <https://doi.org/10.1016/j.geoderma.2015.06.023>, 2016.
- van de Koppel, J., Rietkerk, M., and Weissing, F. J.: Catastrophic vegetation shifts and soil degradation in terrestrial grazing systems, *Trends Ecol. Evol.*, 12, 352-356, 1997.
- Vavrek, M. J.: fossil: palaeoecological and palaeogeographical analysis tools,
825 *Palaeontologia Electronica*, 14, 2011.
- Wang, R., Sun, Y., Zong, J., Wang, Y., Cao, X., Wang, Y., Cheng, X., and Zhang, W.: Remote Sensing Application in Ecological Restoration Monitoring: A Systematic Review, *Remote Sensing*, 16, 2204, 2024.
- 830 Wessels, K. J., Prince, S. D., Malherbe, J., Small, J., Frost, P. E., and VanZyl, D.: Can human-induced land degradation be distinguished from the effects of rainfall variability? A case study in South Africa, *Journal of Arid Environments*, 68, 271-297,
<https://doi.org/10.1016/j.jaridenv.2006.05.015>, 2007.
- Xiao, X., Hagen, S., Zhang, Q., Keller, M., and Moore, B.: Detecting leaf phenology of seasonally moist tropical forests in South America with multi-temporal MODIS
835 images, *Remote Sensing of Environment*, 103, 465-473, 2006.
- Yi, X., Li, G., and Yin, Y.: The impacts of grassland vegetation degradation on soil hydrological and ecological effects in the source region of the Yellow River--A case study in Junmuchang region of Maqin country, *Procedia Environmental Sciences*, 13, 967-981, 2012.
- 840 Yu, H., Xu, J., Okuto, E., and Luedeling, E.: Seasonal response of grasslands to climate change on the Tibetan Plateau, *PLoS One*, 7, e49230, 2012.
- Zeng, C., Zhang, F., Wang, Q., Chen, Y., and Joswiak, D. R.: Impact of alpine meadow degradation on soil hydraulic properties over the Qinghai-Tibetan Plateau, *Journal of Hydrology*, 478, 148-156, <https://doi.org/10.1016/j.jhydrol.2012.11.058>,
845 2013.
- Zhou, W., Yang, H., Huang, L., Chen, C., Lin, X., Hu, Z., and Li, J.: Grassland degradation remote sensing monitoring and driving factors quantitative assessment in China from 1982 to 2010, *Ecological Indicators*, 83, 303-313, 2017.
- 850